# A DFT study of $C_{24}N_{24}$ Fullerene as Anode Material in Li-, Na-, K-, and Mg-Ion Batteries

[1]Shuailing Ma, [1]Junkai Wang*, [2]Zhenxia Huang and [1]Haixin Qi

[1]*School of Materials Science and Engineering, Henan Polytechnic University, Jiaozuo 454003, China.*
[2]*College of Chemistry and Chemical Engineering, Henan Polytechnic University, Jiaozuo 454003, China.*
jkwang@hpu.edu.cn*

**Summary:** The prospective use of $C_{24}N_{24}$ fullerene in Li-, Na-, K-, and Mg-ion batteries (MIBs) was evaluated by density functional theory. The results showed that M-ion (M=Li, Na, K, and Mg) and M-atom were absorbed in the N4 cavity of $C_{24}N_{24}$ fullerene. The storage capacity of Mg-ion batteries (MgIBs) is 516 mAhg$^{-1}$, which is larger than that of Li-, Na-, and K-ion batteries (LIBs, SIBs, and PIBs) with a value of 258 mAgh$^{-1}$. Moreover, the cell voltages for LIBs, SIBs, PIBs, and MgIBs were calculated when $C_{24}N_{24}$ fullerene was used as the anode material. The results of the calculations are -1.75 V, -1.81 V, -2.82 V, and 2.74 V towards LIBs, SIBs, PIBs, and MgIBs, respectively. This research demonstrates that $C_{24}N_{24}$ fullerene may be a useful electrode material for MgIBs.

**Key words:** $C_{24}N_{24}$ fullerene; Density functional theory; Metal-ion batteries; Adsorption; Cell voltage.

## Introduction

Environmental degradation and excessive energy consumption drive the investigations on secondary batteries [1]. Since Li-ion batteries (LIBs) were discovered, they have been broadly applied in various electronic products and automobiles [2, 3]. Although LIBs demonstrate promising performance, there are still some worries about their drawbacks, which include low-voltage energy storage, increased price, and toxicity [2, 4]. Therefore, due to their low cost and wide availability, various additional metal ion batteries, including magnesium-ion (MgIBs), potassium-ion (PIBs), and sodium-ion (SIBs) batteries, have lately attracted the interest of researchers[1,5-8]. However, selecting an acceptable ion battery anode material, on the other hand, remains a difficulty.

Usually, graphite is employed as a material for LIBs anode due to its safety and low cost, but it leads to a low Li capacity (~370 mAgh$^{-1}$)[9]. Other materials have been explored for use as ion battery anode electrodes. For example, graphene and transition metal oxides are suggested as possible LIBs anodes [10-12]. Moreover, Sun *et al.* [13] studied in 2018 phosphorene as a possible MgIBs anode material and obtained a voltage of 0.83 V on average. Xiao *et al.* [1] proposed graphene-like single-layer BSi as a viable anode for LIBs and MgIBs due to its great conductivity, low diffusion energy barriers, and high theoretical capacity.

Recently, there has been lots of interest in porous materials like carbon fullerenes owing to their large specific surface area and outstanding adsorption properties [14-16]. The $C_{24}N_{24}$ fullerene, which can be described as truncated N-doped $C_{60}$ fullerene [17], has a spherical structure similar to $C_{60}$ fullerene [18]. This fullerene is made up of eight s-triazine rings linked together by C-C bonds and features six N4 cavities [19]. Transition metal atom decorated $C_{24}N_{24}$ fullerene has been reported to be a highly active catalyst for the oxidation of CO and $CH_4$[20, 21]. Moreover, Sc and Ti atom coordinated carbon nitride (Sc/Ti@$C_{24}N_{24}$) is also a promising hydrogen storage material [22]. These findings suggest that N4 cavities can provide active sites by forming strong metal-N covalent connections, and no metal atom clustering problems arise across the $C_{24}N_{24}$.

However, there are still few investigations on $C_{24}N_{24}$ fullerene as an electrode material in ion batteries. Therefore, in this report, the possible uses of $C_{24}N_{24}$ fullerene as an electrode for Li-, Na-, K- and Mg-ion batteries were studied by DFT computations in terms of adsorption energy, theoretical capacity, electrical conductivity, cell voltage, and so on. This study has the potential to extend the uses of $C_{24}N_{24}$ fullerene.

---

*To whom all correspondence should be addressed.

*Computational methods*

All computations were completed in DMol$^3$ package [23, 24]. For electron-electron interaction, the generalized gradient approximation (GGA) of the PBE exchange function was adopted [25]. Given the effect of van der Waals force, the DFT-D correction method was used in the calculation [26]. In this study, binary polarization function (DNP) and semi-empirical pseudopotentials (DSPPs) with relativistic correction were adopted for the basis set and kernel electronic method. A convergence tolerance of $1\times10^{-5}$ Ha, $5\times10^{-4}$ nm, and 0.02 Ha·nm$^{-1}$ was used for energy change, maximum displacement, and maximum interaction force, respectively.

In order to compute the adsorption energy ($E_{ad}$) for the Metal atoms or cations interaction with $C_{24}N_{24}$ fullerene, the equation was employed:

$$E_{ad} = E_{M/M^{q+}@C_{24}N_{24}} - E_{C_{24}N_{24}} - E_{M/M^{q+}} \qquad (1)$$

Where $E_{C_{24}N_{24}}$ represents the energy of $C_{24}N_{24}$ fullerene. $E_{M/M^{q+}}$ denotes the energy of a single M

atom or M cation. $E_{M/M^{q+}@C_{24}N_{24}}$ represents the energy of a $C_{24}N_{24}$ that has an attached M atom or M cation.

**Results and discussion**

*Structural optimization*

The optimal geometry of $C_{24}N_{24}$ fullerene is exhibited in Fig.1. As can be seen, it has six N4 cavities similar to porphyrins, and eight s-triazine rings joined by C-C bonds make up each cavity. The C-C and C-N bond distances in $C_{24}N_{24}$ are 1.55 and 1.34 Å, respectively, and they agree with those of other reports [19, 27]. Electronically, the calculations suggest that the $E_g$ of $C_{24}N_{24}$ fullerene is around 0.98 eV, with HOMO and LUMO energies -6.26 and -5.28 eV, respectively (Table-1). Next, the stability of $C_{24}N_{24}$ fullerene is considered. The calculations display that it is more energy-efficient to form $C_{24}N_{24}$ fullerene, and it has the dynamic stability of structure. Moreover, $C_{24}N_{24}$ fullerene can tolerate temperatures as high as 1000 K, which evinces the thermodynamic stability of $C_{24}N_{24}$ fullerene [14].

Table-1: Adsorption energies of atoms and cations on $C_{24}N_{24}$ fullerene ($E_{ad}$), the LUMO, HOMO and LUMO-HOMO gap ($E_g$) for various compounds. Energies are in eV. $\Delta E_g$ denotes the $E_g$ change of the fullerene after atom or cation adsorption. The total energy changes ($\Delta E_{cell}$, eV) and cell voltages ($V_{cell}$) of batteries are shown.

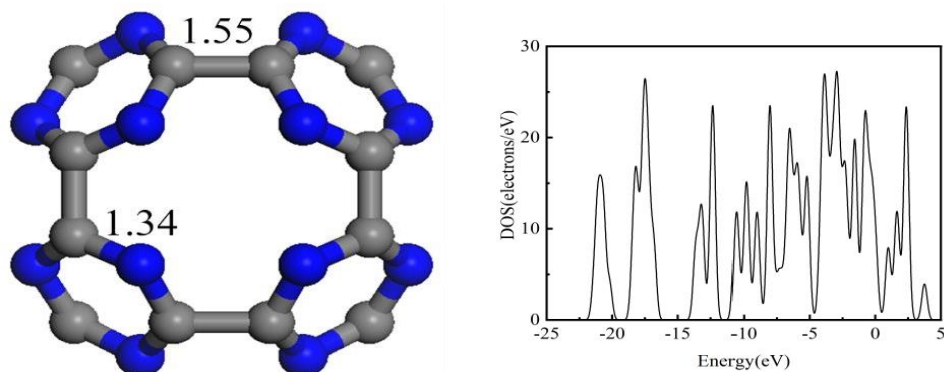| system | $E_{ad}$ | $E_{HOMO}$ | $E_{LUMO}$ | $E_g$ | %$\Delta E_g$ | $\Delta E_{cell}$ | $V_{cell}$ |
|---|---|---|---|---|---|---|---|
| $C_{24}N_{24}$ | — | -6.26 | -5.28 | 0.98 | — | — | — |
| $C_{24}N_{24}$/Li | -5.63 | -6.01 | -5.29 | 0.72 | -26.53 | 1.75 | -1.75 |
| $C_{24}N_{24}$/Li$^+$ | -3.88 | -9.28 | -8.51 | 0.77 | -21.43 | | |
| $C_{24}N_{24}$/Na | -4.58 | -5.79 | -5.08 | 0.71 | -27.55 | 1.81 | -1.81 |
| $C_{24}N_{24}$/Na$^+$ | -2.77 | -9.07 | -8.28 | 0.79 | -19.39 | | |
| $C_{24}N_{24}$/K | -4.70 | -5.61 | -4.89 | 0.72 | -26.53 | 2.82 | -2.82 |
| $C_{24}N_{24}$/K$^+$ | -1.88 | -8.87 | -8.07 | 0.80 | -18.37 | | |
| $C_{24}N_{24}$/Mg | -5.58 | -5.44 | -5.02 | 0.42 | -57.14 | -5.48 | 2.74 |
| $C_{24}N_{24}$/Mg$^{2+}$ | -11.06 | -12.32 | -11.90 | 0.42 | -57.14 | | |



Fig. 1:   Optimized structure of $C_{24}N_{24}$ fullerene and its DOS. Bonds lengths of C-C and C-N bonds are 1.55 and 1.34 Å.

*Adsorption of Li, Na, K, and Mg over the $C_{24}N_{24}$ fullerene*

Metal atoms are believed to be adsorbed on the outer surface of $C_{24}N_{24}$ fullerene. Various adsorption sites on the $C_{24}N_{24}$ surface have been examined, including the top (above the C and N atoms), the bridge positions (above the C-C and C-N bonds), and above the N4 cavity, for finding the lowest-energy configuration for the system. After extensive structural optimization, the most advantageous adsorption site was discovered to be above the N4 cavity. The energies of adsorption are -5.63, -4.58, -4.70, and -5.58 eV for Li@$C_{24}N_{24}$, Na@$C_{24}N_{24}$, K@$C_{24}N_{24}$, and Mg@$C_{24}N_{24}$, respectively. The negative values of $E_{ad}$ show that the complexes have significant stability. What's more, in these configurations, the local structural changes

caused by the adsorption of $C_{24}N_{24}$ fullerene are very small. The C-C and C-N bond lengths in the N4 cavity marginally change from 1.55 and 1.34 Å to 1.54, 1.54, 1.54, 1.52, and 1.36, 1.36, 1.36, 1.38 Å (Table 2) for above complexes (Fig 2), respectively. As shown by the minimal values of structural deformation, the $C_{24}N_{24}$ fullerene maintains its original structure following the metal atoms' adsorption, which is a significant quality for electrode material.

Table-2: The C-C and C-N bond lengths in the N4 cavity of fullerene after atom adsorption (Å).

| System | C-C(Å) | C-N(Å) |
|---|---|---|
| $C_{24}N_{24}$ | 1.55 | 1.34 |
| $C_{24}N_{24}$/Li | 1.54 | 1.36 |
| $C_{24}N_{24}$/Na | 1.54 | 1.36 |
| $C_{24}N_{24}$/K | 1.54 | 1.36 |
| $C_{24}N_{24}$/Mg | 1.52 | 1.38 |



(a)                   (b)

(c)                   (d)
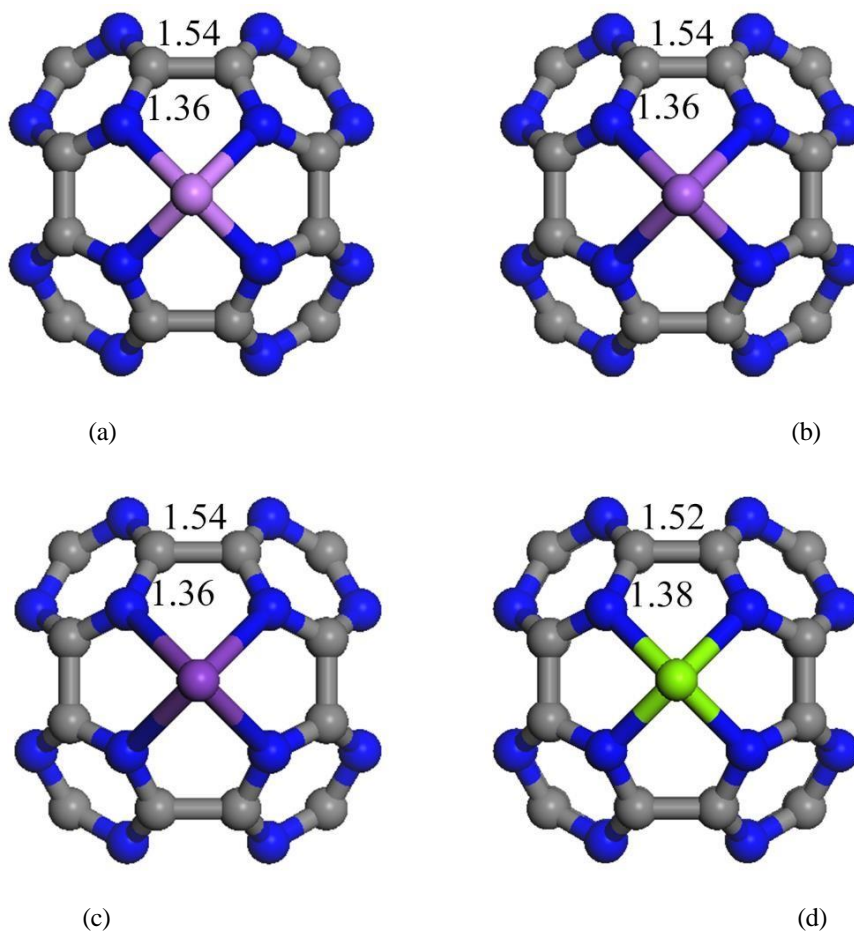
Fig. 2: Structural changes after adsorption of atoms. (a) Li@$C_{24}N_{24}$, (b) Na@$C_{24}N_{24}$, (c) K@$C_{24}N_{24}$, (d) Mg@$C_{24}N_{24}$.
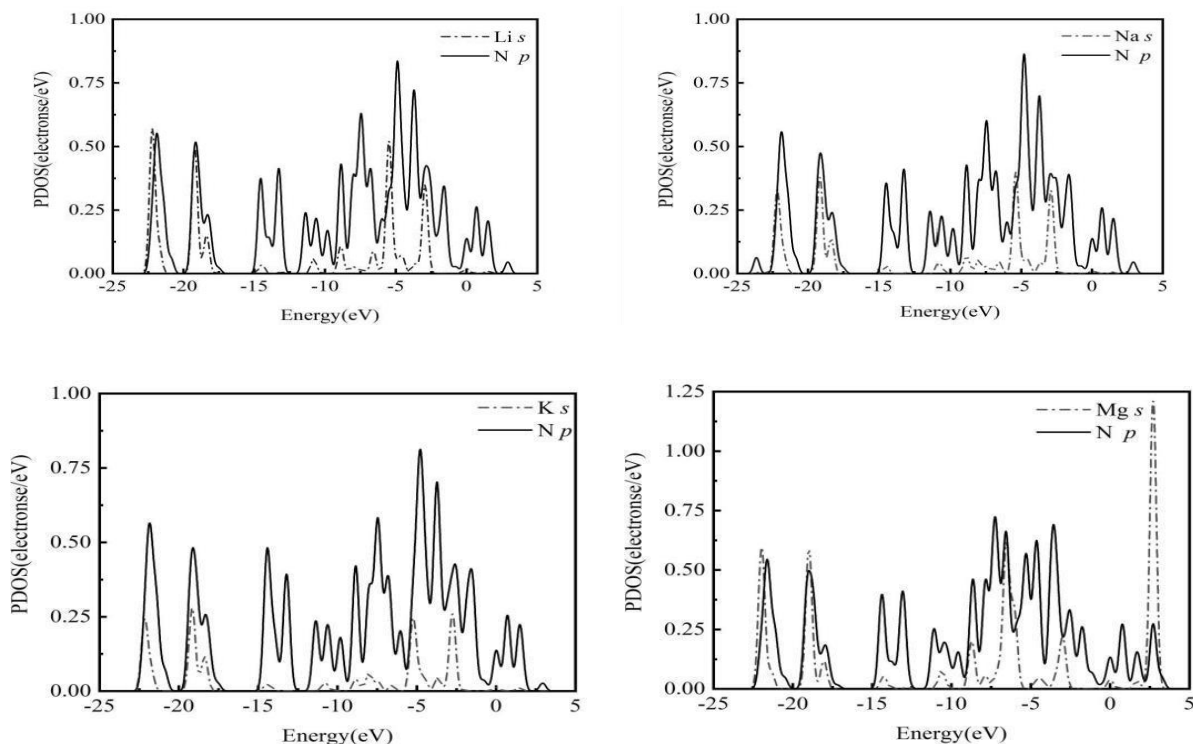
Fig. 3:    Partial density of states (PDOS) plots of $C_{24}N_{24}$ system after Li, Na, K, Mg atom adsorption.

In this paper, the PDOS plots for metal-adsorbed $C_{24}N_{24}$ fullerene have been drawn, as shown in Fig 3. The PDOS plots show that there is a significant overlap between the metal atom and $C_{24}N_{24}$ fullerene states around the Fermi-level. This supports the better stability and stronger metal atom adsorption on the N4 cavity of $C_{24}N_{24}$ fullerene.

*Adsorption of $Li^+$, $Na^+$, $K^+$, and $Mg^{2+}$ over the $C_{24}N_{24}$ fullerene*

To explore the metal cation's adsorption on the $C_{24}N_{24}$ fullerene, it was put on different sites, and much like with metal atoms, one local minimum was discovered. The calculations display that when a metal cation is put on a C-N bond or a carbon atom of $C_{24}N_{24}$, it moves above the N4 cavity of $C_{24}N_{24}$ fullerene, as demonstrated in Fig 4.

According to Table-1, the $Mg^{2+}$ adsorption energy on $C_{24}N_{24}$ fullerene is -11.06 eV, which is stronger than for the Mg atom (-5.58 eV). This shows that because of the great charge concentration of $Mg^{2+}$, there is a large interaction between $Mg^{2+}$ and $C_{24}N_{24}$ fullerene, while the association with the Mg atom is modest. It should be noted also that the adsorption energies of $Li^+/Na^+/K^+$ on $C_{24}N_{24}$ fullerene are weaker

than those of Li/Na/K atoms; this is opposite compared to the adsorption of $Mg/Mg^{2+}$. Thus, the $C_{24}N_{24}$ fullerene is predicted to be only applicable to one of the Li/Na/K/Mg-ion batteries, possibly, but not all of them.

To consider how cation adsorption affects the electrical characteristics of $C_{24}N_{24}$ fullerene, the results of energy gap ($E_g$) have been calculated as shown in Table-1. In these stable complexes, after $Mg^{2+}$ adsorption, the $E_g$ of $C_{24}N_{24}$ is reduced significantly (by about 57.14%) compared to the $Li^+$, $Na^+$, and $K^+$ adsorption (about 21.43%, 19.39%, 18.37%). What's well known is that the electrical conductivity of a material is mostly determined by $E_g$; at a given temperature, smaller $E_g$ values might result in higher conductance [28, 29]. As a result, the reduction in $E_g$ following adsorption causes a change in the electrical conductivity of $C_{24}N_{24}$ fullerene. Beyond this, the internal electronic resistance of the battery can be reduced by better electron conductivity. This is also a significant component influencing battery performance because it can minimize the formation of Joule heat during charging and discharging. Thus, $C_{24}N_{24}$ fullerene is more appropriate for application as an Mg-ion battery electrode because of its higher electrical conductivity.
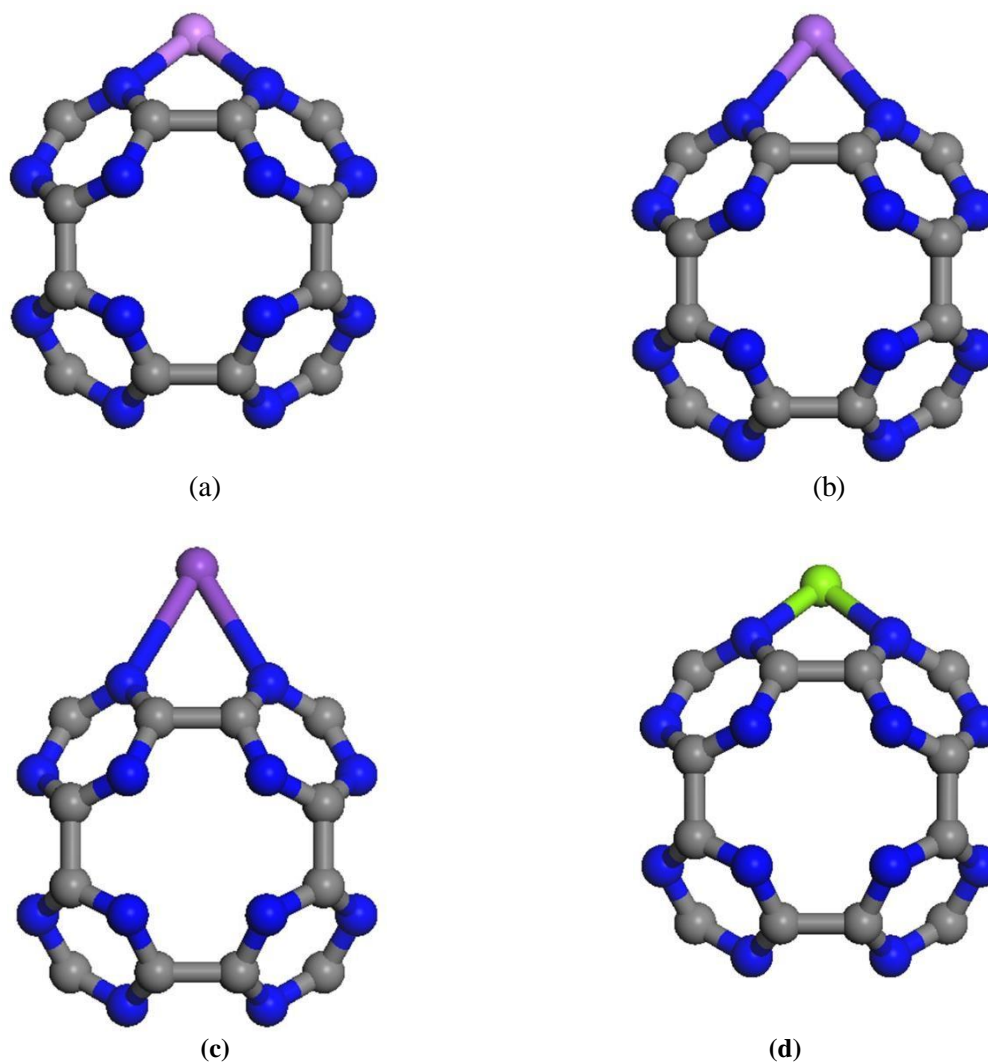
(a)　　　　　　　　　　　　　　　　　　　(b)

(c)　　　　　　　　　　　　　　　　　　　(d)

Fig. 4:　Optimized structures of (a) $Li^+@C_{24}N_{24}$, (b) $Na^+@C_{24}N_{24}$, (c) $K^+@C_{24}N_{24}$, (d) $Mg^{2+}@C_{24}N_{24}$.

*Theoretical capacity of $C_{24}N_{24}$ fullerene*

Next, the theoretical capacity of $C_{24}N_{24}$ fullerene was calculated. It is one of the most important variables to consider while researching battery performance. The following expression can be used to calculate theoretical capacity.

$$C = \frac{(n_{max} qF)}{M_{C_{24}N_{24}}} \qquad (2)$$

Where $n_{max}$, $q$, $F$, and $M_{C_{24}N_{24}}$ are the maximum number of adsorbed metal atoms, valence electron number, Faraday constant ($26.81 Ahmol^{-1}$), and molar mass of $C_{24}N_{24}$ fullerene, respectively. The current results show that even after adsorbing six metal atoms, the $C_{24}N_{24}$ fullerene can maintain its geometry. In this
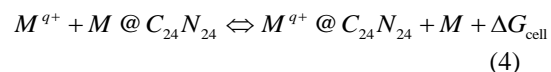
study, the theoretical capacity of $C_{24}N_{24}$ fullerene towards Li/Na/K and Mg are 258 and 516 $mAhg^{-1}$ (based on $Li_6C_{24}N_{24}$, $Na_6C_{24}N_{24}$, $K_6C_{24}N_{24}$, and $Mg_6C_{24}N_{24}$). In comparison, the theoretical Mg capacity is much larger than that of $g$-$C_3N_4$ (319.2 $mAgh^{-1}$) [30] and close to that of $C_2N$ (588.4 $mAgh^{-1}$) [30]. On the contrary, the theoretical Li/Na/K capacities of $C_{24}N_{24}$ fullerene are lower compared with some anode materials. For instance, the theoretical Li capacity of $C_{24}N_{24}$ fullerene is smaller than that of $Ti_3C_2$ (447.8 $mAgh^{-1}$) [31] and $B_2C$ (1596 $mAgh^{-1}$) [32]. The theoretical Na capacity of $C_{24}N_{24}$ fullerene is much lower than that of graphene (1117 $mAgh^{-1}$) [33] and $B_2C$ (1596 $mAgh^{-1}$) [32]. Thus, $C_{24}N_{24}$ fullerene has the potential as electrode material for Mg-ion batteries.

*Cell voltage*

Voltage is another crucial criterion for evaluating the effectiveness of batteries. A high voltage can lead to a great specific energy storage capacity and a large energy density, both of which are crucial factors for describing how well an ion battery performs. If $C_{24}N_{24}$ is utilized as an anode for batteries, the reaction formula of the anode and cathode can be defined as:

$$M @ C_{24}N_{24} \Leftrightarrow M^{q+} @ C_{24}N_{24} + qe^- \; (anode) \quad M^{q+} + qe^- \Leftrightarrow M \; (cathode)$$

(3)
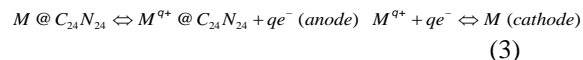
The overall reaction can be defined as:

$$M^{q+} + M @ C_{24}N_{24} \Leftrightarrow M^{q+} @ C_{24}N_{24} + M + \Delta G_{cell}$$

(4)

The following equation is used to obtain the cell voltage:

$$V_{cell} = -\Delta G_{cell} / zF$$

(5)

$$\Delta G_{cell} = \Delta E_{cell} + P\Delta V_{cell} - T\Delta S_{cell}$$

(6)

The volume and entropy make little contributions to cell voltage and have little to no impact on it (less than 0.01 V) [34]. Thus, excluding the terms $P\Delta V_{cell}$ and $T\Delta S_{cell}$, the formula can be written as:

$$\Delta E_{cell} \square \Delta G_{cell} = E(M) + E(M^{q+} @ C_{24}N_{24}) - E(M^{q+}) - E(M @ C_{24}N_{24})$$

(7)

According to this equation, $\Delta E_{cell}$ will get more negative and larger as the $M^{q+}$ interaction with $C_{24}N_{24}$ fullerene becomes stronger. In other words, a high voltage might result from the strong $M^{q+}$ adsorption and weak M adsorption on the $C_{24}N_{24}$ fullerene. As discussed above, compared to the Mg atom, the $Mg^{2+}$ adsorption on the $C_{24}N_{24}$ fullerene is significantly greater in the Mg-ion battery. Thus, this may result in a high cell voltage. The calculations indicate that $\Delta E_{cell}$ and voltage values are predicted to be around -5.48 eV and 2.74 V. As a comparison, the voltage value is greater than that with phosphorene (~0.83 V)[13]. Therefore, it has potential as an electrode for Mg-ion battery. However, when $C_{24}N_{24}$ is applied as an electrode for Li/Na/K-ion batteries, it ought to be noted that the Li/Na/K atom adsorption is greater than that of $Li^+/Na^+/K^+$. The computed $\Delta E_{cell}$

and cell voltage values are 1.75, 1.81, 2.82 eV and -1.75, -1.81, -2.82 V, respectively. These suggest that the cell voltage generated by the $C_{24}N_{24}$ fullerene in K-ion batteries is close to that in Mg-ion batteries. However, considering the electrical conductivity and theoretical capacity factors, $C_{24}N_{24}$ fullerene is more suitable for Mg-ion battery electrode material.

## Conclusions

The adsorption of $M^{q+}$ and M on $C_{24}N_{24}$ fullerene was investigated to examine its possible application as an anode of Li/Na/K/Mg-ion batteries. The results show that the $C_{24}N_{24}$ fullerene has excellent electrical conductivity after the adsorption of $Mg^{2+}$ cation. The storage capacity of $C_{24}N_{24}$ fullerene anode for MgIBs can reach up to 516 mAhg$^{-1}$, which is larger than that of LIBs, SIBs, and PIBs with the value of 258 mAgh$^{-1}$. The cell voltage generated by the $C_{24}N_{24}$ fullerene in MgIBs is 2.74 V. As comparison, the cell voltage of MgIBs is much higher than that of LIBs (-1.75 V) and SIBs (-1.81 V), and close to that of PIBs (-2.82 V). These results suggest that $C_{24}N_{24}$ fullerene is appropriate as an anode of MgIBs.

## Acknowledgements

## References

1. C. Xiao, X. Tang and J. Peng. Graphene-like BSi as a promising anode material for Li-and Mg-ion batteries: A first principle study. *Appl. Surf. Sci.*, **563**, 150278 (2021).

2. H. M. Berenjaghi, S. Mansouri and J. Beheshtian. A DFT study on the potential application of pristine, B and N doped carbon nanocones in potassium-ion batteries. *J. Mol. Model.*, **27**, 1 (2021).

3. J. P. Rivera-Barrera, N. Muñoz-Galeano and H. O. Sarmiento-Maldonado. SoC estimation for lithium-ion batteries: Review and future challenges. *Electronics*, **6**, 102 (2017).

4. X. Wu, J. Wang and D. Fei. Lithium metal anodes for rechargeable batteries. *Energy Environ. Sci.*, **7**, 513 (2014).

5. Y. Zhang, J. Qin and S. E. Lowe. Enhanced electrochemical production and facile modification of graphite oxide for cost-effective sodium ion battery anodes. *Carbon*, **177**, 71 (2021).

6. W. Pei, H. Long and X. Zhang. AlN nanotubes and nanosheets as anode material for K-ion batteries:

DFT studies. *Phys. Lett. A*, **384**, 126396 (2020).

7.  E. Vessally, I. Alkorta and S. Ahmadi. A DFT study on nanocones, nanotubes (4, 0), nanosheets and fullerene $C_{60}$ as anodes in Mg-ion batteries. *RSC Adv.*, **9**, 853 (2019).

8.  T. Hussain, E. Olsson and K. A. Alhameedi. Functionalized two-dimensional nanoporous graphene as efficient global anode materials for Li-, Na-, K-, Mg-, and Ca-ion batteries. *J. Phys. Chem. C*, **124**, 9734 (2020).

9.  J. R. Dahn, T. Zheng and Y. Liu. Mechanisms for lithium insertion in carbonaceous materials. *Science*, **270**, 590 (1995).

10. J. Hassoun, F. Bonaccorso and M. Agostini. An advanced lithium-ion battery based on a graphene anode and a lithium iron phosphate cathode. *Nano Lett.*, **14**, 4901 (2014).

11. X. Yuan, X. Li. Vanadium Hexacyanoferrate Derived V-Fe-K Mixed Oxides as Anode Materials for Lithium-Ion Batteries. *ChemistrySelect*, **5**, 13748 (2020).

12. Q. Ren, Y. Zhang and C. Liu. Hollow-sphere iron oxides exhibiting enhanced cycling performance as lithium-ion battery anodes. *ChemComm*, **55**, 11638 (2019).

13. X. Han, C. Liu and J. Sun. Density functional theory calculations for evaluation of phosphorene as a potential anode material for magnesium batteries. *RSC Adv.*, **8**, 7196 (2018).

14. A. A. Khan, R. Ahmad and I. Ahmad. Selective adsorption of $CO_2$ from gas mixture by P-decorated $C_{24}N_{24}$ fullerene assisted by an electric field: A DFT approach. *J. Mol. Graph. Model.*, **103**, 107806 (2021).

15. H. R. Karfunkel, T. Dressler and A. Hirsch. Heterofullerenes: structure and property predictions, possible uses and synthesis proposals. *J. Comput. Aided Mol. Des.*, **6**, 521 (1992).

16. Y. Fujimoto, S. Saito. Hydrogen adsorption and anomalous electronic properties of nitrogen-doped graphene. *J. Appl. Phys.*, **115**, 153701 (2014).

17. E. Shakerzadeh, E. Tahmasebi and M. Solimannejad. Tuning the electronic-optical properties of porphyrin-like porous $C_{24}N_{24}$ fullerene with $(Li_3O)$ n=(1-5) decoration. A computational study. *Appl Organomet Chem*, **33**, e4654 (2019).

18. M. Prato. [60] Fullerene chemistry for materials science applications. *J. Mater. Chem. A*, **7**, 1097 (1997).

19. K. Srinivasu, S. K. Ghosh. Transition metal decorated porphyrin-like porous fullerene: promising materials for molecular hydrogen adsorption. *J. Phys. Chem. C*, **116**, 25184 (2012).

20. E. Shakerzadeh, H. Hamadi and M. D. Esrafili. Computational mechanistic insights into CO oxidation reaction over Fe decorated $C_{24}N_{24}$ fullerene. *Inorg Chem Commun*, **106**, 190 (2019).

21. P. Mousavian, M. D. Esrafili. Methane oxidation into methanol catalyzed by TM-anchored $C_{24}N_{24}$ nanoclusters (TM= Fe, Co and Ni): A DFT study. *Inorg Chem Commun*, **122**, 108317 (2020).

22. L. J. Ma, W. Hao and T. Han. Sc/Ti decorated novel $C_{24}N_{24}$ cage: Promising hydrogen storage materials. *Int. J. Hydrog. Energy*, **46**, 7390 (2021).

23. B. Delley. An all-electron numerical method for solving the local density functional for polyatomic molecules. *J. Chem. Phys.*, **92**, 508 (1990).

24. B. Delley. From molecules to solids with the $DMol^3$ approach. *J. Chem. Phys.*, **113**, 7756 (2000).

25. J. P. Perdew, K. Burke and M. Ernzerhof. Generalized gradient approximation made simple. *Phys. Rev. Lett.*, **77**, 3865 (1996).

26. S. Grimme. Accurate description of van der Waals complexes by density functional theory including empirical corrections. *J Comput Chem*, **25**, 1463 (2004).

27. M. D. Esrafili, S. Hosseini. Reversible $CO_2$ storage and efficient separation using Ca decorated porphyrin-like porous $C_{24}N_{24}$ fullerene: a DFT study. *RSC Adv.*, 11, 34402 (2021).

28. S. S. Li. Scattering mechanisms and carrier mobilities in semiconductors//Semiconductor Physical Electronics. *Springer*, New York, NY, 211 (2006).

29. A. A. Peyghan, M. Noei. A theoretical study of lithium-intercalated pristine and doped carbon nanocones. *J. Am. Chem. Soc.*, **58**, 46 (2014).

30. J. Zhang, G. Liu and H. Hu. Graphene-like carbon-nitrogen materials as anode materials for Li-ion and mg-ion batteries. *Appl. Surf. Sci.*, **487**: 1026 (2019).

31. D. Er, J. Li and M. Naguib. $Ti_3C_2$ MXene as a high capacity electrode material for metal (Li, Na, K, Ca) ion batteries. *ACS Appl. Mater. Interfaces*, **6**, 11173 (2014).

32. X. Yu, X. Chen and X. Wang. Metallic $B_2C$ monolayer as a promising anode material for Li/Na ion storage. *Chem. Eng. J.*, **406**, 126812 (2021).

33. Z. Liang, X. Fan and W. Zheng. Adsorption and formation of small Na clusters on pristine and double-vacancy graphene for anodes of Na-ion batteries. *ACS Appl. Mater. Interfaces*, **9**, 17076 (2017).

34. Y. S. Meng, M. E. Arroyo-de Dompablo. First principles computational materials design for energy storage materials in lithium ion batteries. *Energy Environ. Sci.*, **2**, 589 (2009).